Color Point Tuning for $(Sr,Ca,Ba)Si_2O_2N_2:Eu^{2+}$ for White Light LEDs

Volker Bachmann,[†,‡] Cees Ronda,[†,‡,§] Oliver Oeckler,[||] Wolfgang Schnick,[||] and Andries Meijerink*[,‡]

Philips Technologie GmbH Research Laboratories, Weisshausstrasse 2, D-52066 Aachen, Germany, Department of Condensed Matter, Debye Institute, Utrecht University, P.O. Box 80 000, 3508 TA Utrecht, The Netherlands, Centre for Optical and Electromagnetic Research, Zhejiang University, Hangzhou 310058, China, and Department Chemie and Biochemie, Lehrstuhl für Anorganische Festkörperchemie, Ludwig-Maximilians-Universität München, Butenandtstrasse 5-13 (D), 81377 München, Germany

Received September 8, 2008. Revised Manuscript Received November 5, 2008

Color point tuning is an important challenge for improving white light LEDs. In this paper, the possibilities of color tuning with the efficient LED phosphor $Sr_{1-x-y-z}Ca_xBa_ySi_2O_2N_2:Eu_z^{2+}$ ($0 \le x, y \le 1$; $0.005 \le z \le 0.16$) are investigated. The emission color can be tuned in two ways: by changing Eu^{2+} concentration and by substitution of the host lattice cation Sr^{2+} by either Ca^{2+} or Ba^{2+}. The variation in the Eu^{2+} concentration shows a red shift of the emission upon increasing the Eu concentration above 2%. The red shift is explained by energy migration and energy transfer to Eu^{2+} ions emitting at longer wavelengths. Along with this (desired) red shift there is an (undesired) lowering of the quantum efficiency and the thermal quenching temperature due to concentration quenching. Partial substitution of Sr^{2+} by either Ca^{2+} or Ba^{2+} also results in a red-shifted Eu^{2+} emission. For Ca^{2+} this is expected and the red shift is explained by an increased crystal field splitting for Eu^{2+} on the (smaller) Ca^{2+} cation site. For Ba^{2+}, the red shift is surprising. Often, a blue shift of the fd emission is observed in case of substitution of Sr^{2+} by the larger Ba^{2+} cation. The Eu^{2+} emission in the pure $BaSi_2O_2N_2$ host lattice is indeed blue-shifted. Temperature dependent luminescence measurements show that the quenching temperature drops upon substitution of Sr by Ca, whereas for Ba substitution, the quenching temperature remains high. Color tuning by partial substitution of Sr^{2+} by Ba^{2+} is therefore the most promising way to shift the color point of LEDs while retaining the high quantum yield and high luminescence quenching temperature.

1. Introduction

The market for white-light-emitting LEDs is expanding rapidly. From niche applications, like flashlights and traffic lights, white light LEDs are now finding their way into general lighting applications and are expected to be found in every home soon. This has an impact on research on luminescent materials (phosphors). Research on phosphors for lighting used to be focused on the conversion of 254 nm UV radiation from a mercury discharge into visible light. Today, these phosphors, used in fluorescent tubes, are mature products that are stable and highly efficient (90% quantum efficiency).[1] Present work aims at incremental improvements in efficiency, morphology, price, and stability of existing phosphors. With the invention of the near-UV to blue-emitting GaN-based LEDs by Nakamura in 1991 and the development of high-power LEDs (HP-LEDs)[2] in the same spectral region, the need for new phosphors arose. These phosphors have to efficiently absorb in the near UV to blue spectral range and emit light in the visible. The energy difference between excitation and emission wavelength is small, which is good for the energy efficiency, but it lowers the choice of activator ions that can be used and at present research is mainly focused on Eu^{2+} and Ce^{3+}. For an LED phosphor to be applied in commercial products, several criteria have to be met such as high efficiency in light conversion, high thermal quenching temperature, and the possibility to adjust the color point by means of varying the chemical composition. Host lattices with a high degree of covalency and/or a large crystal field splitting at the site for which Ce^{3+} or Eu^{2+} substitute can lead to efficient visible emission while absorbing light in the near UV to blue range of the electromagnetic spectrum. Presently oxides like $Y_3Al_5O_{12}:Ce^{3+}$ or sulfides like $CaS:Eu^{2+}$ are applied in phosphor converted LEDs (pc-LEDs) as luminescent converters.[3,4]

An important property of white light LEDs is the color temperature. The combination of blue light from the LED and the yellow emission from the most widely applied YAG:Ce phosphor gives a relatively cool white light. For general

* Corresponding author. E-mail: a.meijerink@uu.nl. Tel.: 31 (0) 30-253 2202. Fax: 31 (0) 30-253 2403.
† Philips Technologie GmbH Research Laboratories.
‡ Utrecht University.
§ Zhejiang University.
|| Ludwig-Maximilians-Universität München.

(1) Blasse, G.; Grabmaier B. C. *Luminescent Materials*; Springer Verlag: Berlin, 1994.
(2) (a) Nakamura, S. *Jpn. J. Appl. Phys* **1991**, *30* (10A), L1705. (b) Nakamura, S.; Fasol, G. *The Blue Laser Diode: GaN Based Light Emitters and Lasers*; Springer: Berlin, 1997; p 343.
(3) Schlotter, P.; Baur, J.; Hielscher, Ch.; Kunzer, M.; Obloh, H.; Schmidt, R.; Schneider, J. *Mater. Sci. Eng., B* **1999**, *59*, 390.
(4) Hu, Y.; Zhuang, W.; Ye, H.; Zhang, S.; Fang, Y.; Huang, X. *J. Lumin.* **2005**, *111*, 139.

10.1021/cm802394w CCC: $40.75
Published on Web 12/29/2008

lighting applications it is essential to make pc-LEDs that emit a warmer white light. A shift to the orange/red spectral region is needed to realize this. In addition, the efficiency of primary LEDs in the yellow is low and the development and color tuning of yellow/green pc-LEDs is an important challenge as these pc-LEDs offer the possibility of efficiencies five times higher than for primary LEDs in this spectral region. In this respect, a promising new class of LED phosphor materials is the oxonitridosilicates, known as sions. The N^{3-} in this lattice is a soft Lewis base, which results in a high covalency. This shifts the energy of the 4f−5d absorption and emission for Eu^{2+} and Ce^{3+} ions in these host lattices to sufficiently low energies. In addition, sions are known to be highly stable toward oxidation and hydrolysis.[5] We, among others, reported recently on $SrSi_2O_2N_2$:Eu^{2+}.[6−10] For this lattice, the Eu^{2+} absorption and emission are in the visible range of the spectrum. The material was developed earlier in a synthesis approach leading to the highly efficient nitridosilicate phosphor $M_2Si_5N_8$:Eu^{2+} (M = Sr, Ba).[11,12] The conversion efficiency, determined as relative quantum efficiency, is greater than 90% and the thermal quenching temperature for the emission is high. Yun et al. and Mueller-Mach et al. reported on the use of $SrSi_2O_2N_2$:Eu^{2+} and $M_2Si_5N_8$:Eu^{2+} (M = Ca, Sr, Ba) in pc-LEDs[13] and showed that these materials are promising for application in warm-white pc-LEDs.

In this paper we report on the possibility to tune the emission color for the LED phosphor $SrSi_2O_2N_2$:Eu^{2+} in two different ways: first by varying the concentration of the Eu^{2+} dopant and second by replacing Sr^{2+} (partly or completely) by Ca^{2+} or Ba^{2+}. Structural changes, luminescence quenching temperatures and quantum efficiencies were examined to determine the influence of doping $SrSi_2O_2N_2$:Eu^{2+}. Temperature-dependent luminescence and decay time measurements were performed to understand the mechanisms responsible for the color change and the quenching behavior and to determine the most promising way to design new compositions that can serve as efficient phosphors in pc-LEDs with a warmer color.

2. Experimental Section

Samples were synthesized using a conventional solid-state reaction. As starting materials were used: $SrCO_3$ (Philips Lighting Components, 99.9%), $CaCO_3$ (Philips Lighting Components, 99.9%), $BaCO_3$ (Philips Lighting Components, 99.9%), $Si_3N_{4-x}(NH)_{3/2x}$ ($x \approx 1$, made by thermal decomposition of $Si(NH)_2$, O content < 2 wt %), and the rare earth dopant Eu_2O_3 (Alfa Aesar, REacton 99.999%). Mixtures of these materials were prepared by ball milling and firing for 2−4 h at 1200−1500 °C in a reducing atmosphere (H_2/N_2) in a tube furnace. Working in a reducing atmosphere and being doped to a divalent lattice site, europium will be built into the host lattice as Eu^{2+}. After being milled, the raw product powders were washed with water and isopropanol. XRD analysis was done on a Philips diffractometer PW 1729 at RT, using Cu Kα radiation. For the samples with a partial substitution of Sr^{2+} with Ca^{2+} or Ba^{2+}, a shift in the lines in the diffraction pattern is observed because of a change in the lattice constants.

Luminescence spectra were recorded between 4 and 300 K on a Spex Fluorolog 2 spectrofluorimeter equipped with a helium flow cryostat. To study thermal quenching between 300 and 600 K the same spectrofluorimeter was equipped with a homemade heating cell. Both types of measurements used a Xe-lamp as excitation source. The spectra were measured with a spectral resolution of 0.5 to 1.0 nm. On a different setup quantum efficiencies were measured relative to a sample of YAG:Ce from which the absolute quantum efficiency is known to be 70%. The quantum efficiencies were measured relative to externally calibrated standards. First we measured the reflection of black velvet (with reflectivity 3%) and $BaSO_4$ (reflectivity 99%). This enabled us to calculate the reflection of the phosphors investigated, including the standard phosphors. The emission spectra of the phosphors investigated were integrated over the wavelength, this gave the relative number of photons emitted for each of the phosphors. This enabled us to calculate the quantum efficiencies of the phosphors, using the known quantum efficiency values for the standard phosphors used.

Luminescence lifetime measurements were done using the third harmonic (355 nm) of a Quanta-ray DCR YAG:Nd laser as the excitation source. Luminescence decay curves were measured using a 0.25 m Acton Research monochromator and an RCA C31034 photomultiplier tube in combination with a Tektronix 2430 Digital Oscilloscope. For temperature-dependent measurements, the same type of cryostat and heating cell as described above are used.

3. Results and Discussion

3.1. Crystal Structures. The phase purity of the end compositions $CaSi_2O_2N_2$, $SrSi_2O_2N_2$, and $BaSi_2O_2N_2$ were checked using X-ray powder diffraction. For the first two compositions, precise structure analyses have been published.[14,15] The structures of the two materials are similar but not isotypic. They were found to consist of alternating layers of Ca^{2+} or Sr^{2+} and layers with composition $[Si_2O_2N_2]^{2-}$. These layers exhibit orthorhombic symmetry and consist of $SiON_3$-tetrahedrons that are condensed via N atoms bridging three of the Si atoms each, whereas the O atoms are terminally bound to the Si atom. In the Ca and Sr compounds, these O-atom vertices point up and down from the layers in a different fashion. The O atoms coordinate

(5) Schnick, W. *Int. J. Inorg. Mater.* **2001**, *3*, 1267.
(6) Bachmann, V.; Jüstel, T.; Meijerink, A.; Ronda, C. R.; Schmidt, P. J. *J. Lumin.* **2006**, *121*, 441.
(7) (a) Delsing, A. C. A.; Hintzen, H. T.; Li, Y.-Q. World Patent WO 2003/030923, A1. (b) Schmidt, P. J.; Jüstel, T.; Mayr, W.; Bausen, H.-D.; Schnick, W.; Höppe, H. World Patent WO 2004/036962, A1.
(8) Tamaki, H.; Kakashima, S. World Patent WO 2004/039915, A1.
(9) Fiedler, T.; Jermann, F. World Patent WO 2005/030905, A1.
(10) Li, Y. Q.; Delsing, A. C. A.; de With, G.; Hintzen, H. T. *Chem. Mater.* **2005**, *17*, 3242.
(11) (a) Schlieper, T.; Milius, W.; Schnick, W. *Z. Anorg. Allg. Chem* **1995**, *621*, 1380. Huppertz, H.; Schnick, W. *Acta Crystallogr., Sect. C* **1997**, *53*, 1751. (b) Höppe, H. A.; Lutz, H.; Morys, P.; Schnick, W.; Seilmeier, A. *J. Phys. Chem. Solids* **2000**, *61*, 2001.
(12) (a) Piao, X.; Horikawa, T.; Hanzawa, H.; Machida, K.-I. *Appl. Phys. Lett.* **2006**, *88* (16), 161908–1. (b) Li, Y. Q.; van Steen, J. E. J.; van Krevel, J. W. H.; Botty, G.; Delsing, A. C. A.; DiSalvo, F. J.; de With, G.; Hintzen, H. T. *J. Alloys Compd.* **2006**, *417*, 273. (c) Xie, R.-J.; Hirosaki, N.; Suehiro, T.; Xu, F.-F.; Mitomo, M. *Chem. Mater.* **2006**, *18*, 5578.
(13) (a) Mueller-Mach, R.; Mueller, G.; Krames, M. R.; Höppe, H. A.; Stadler, F.; Schnick, W.; Juestel, T.; Schmidt, P. J. *Phys. Status Solidi (A)* **2005**, *202*, 1727. (b) Yun, B.-G.; Miyamoto, Y.; Yamamoto, H. *J. Electrochem. Soc.* **2007**, *154* (10), J320.
(14) Oeckler, O.; Stadler, F.; Rosenthal, T.; Schnick, W. *Solid State Sci.* **2007**, *9*, 205.
(15) Höppe, H. A.; Stadler, F.; Oeckler, O.; Schnick, W. *Angew. Chem.* **2004**, *116*, 5656. (a) Angew. Chem., Int. Ed. 2004,*43*,5540.

the divalent cations Ca and Sr, which themselves form pseudohexagonal layers. There are four different Ca^{2+} and Sr^{2+} crystallographic sites in the lattice. $CaSi_2O_2N_2$ was found to have a monoclinic unit cell with lattice parameters a = 732.4(2) pm, b = 1365.6(3) pm, c = 1048.3(2) pm, β = 102.04(3)°. It belongs to space group $P2_1$ (No. 4). $SrSi_2O_2N_2$ was found to have a triclinic unit cell with the lattice parameters a = 708.02(2) pm, b = 723.06(2) pm, c = 725.54(2) pm, α = 88.767(3)°, β = 84.733(2)°, γ = 75.905(2)°. It belongs to space group $P1$ (No. 1). The low symmetry arises from the combination of the orthorhombic silicate layers with pseudohexagonal metal atom layers.

For $BaSi_2O_2N_2$, structural investigations show that this compound has a layered structure like the two materials described above,[16] and the configuration of the layers is comparable to that in $SrSi_2O_2N_2$. It exhibits an orthorhombic unit cell with the lattice parameters a = 533.5(3) pm, b = 482.9(2) pm, c = 1437.8(7) pm. Despite a certain degree of disorder, there is only one crystallographic site for Ba^{2+} in the structure, which can be described as a cuboid. This will have an impact on the luminescence spectra, which will be discussed later.

The X-ray diffraction patterns that were recorded for the various compositions of $Sr_{1-x-y-z}Ca_xBa_ySi_2O_2N_2:Eu_z^{2+}$ ($0 \le x, y \le 1$; $0.005 \le z \le 0.16$) are consistent with the crystal structures described above. For codoping Ba or Ca in $SrSi_2O_2N_2$, a small shift in the diffraction peaks is observed because of a change in the lattice parameters as a result of the difference in ionic radius of Ca (smaller) or Ba (larger) with respect to Sr. There is also evidence for the formation of byproducts, which also implies that the actual amounts of Ba, Sr, and Ca incorporated in $Sr_{1-x-y-z}Ca_xBa_ySi_2O_2N_2$ may deviate somewhat from the amounts present in the starting materials. The X-ray diffraction patterns will be shown and discussed in detail in connection with the luminescence properties below.

3.2. $Sr_{1-x}Eu_xSi_2O_2N_2$. The influence of the Eu^{2+} concentration on the luminescence properties was investigated by varying the Eu concentration between 0.5 and 16%. Figure 1(a) shows the excitation, emission, and reflection spectrum at room temperature for the sample with 2% Eu^{2+}. As can be seen from the reflection spectrum, the host material doped with Eu^{2+} shows strong absorption in the blue spectral range of the spectrum which is consistent with a yellow daylight color. Excitation at 450 nm gives a green band emission centered around 539 nm. The emission band is assigned to the $4f^65d^1 \rightarrow 4f^7$ (5d−4f) transition on Eu^{2+}. It differs in position and width from the emission band reported for $Sr_2Si_2O_{2-\delta}N_{2+2/3\delta}:Eu^{2+}$ ($\delta \approx 1$) with the same XRD pattern.[10] This is partly due to the higher Eu^{2+} concentration (10%) in the case of ref 10. However, when comparing our highest doped sample (16% vs 10% in ref 10) still a further red shift of the emission maximum as well as a pronounced shoulder on the low energy side of the spectrum in ref 10 is noticed. This has a significant influence on the position of the color point in the CIE chromaticity coordinate diagram. Possibly this shift and the shoulder originate from traces of $Sr_2Si_5N_8:Eu^{2+}$, a red emitting phosphor,[11−13] in the samples reported in ref 10.

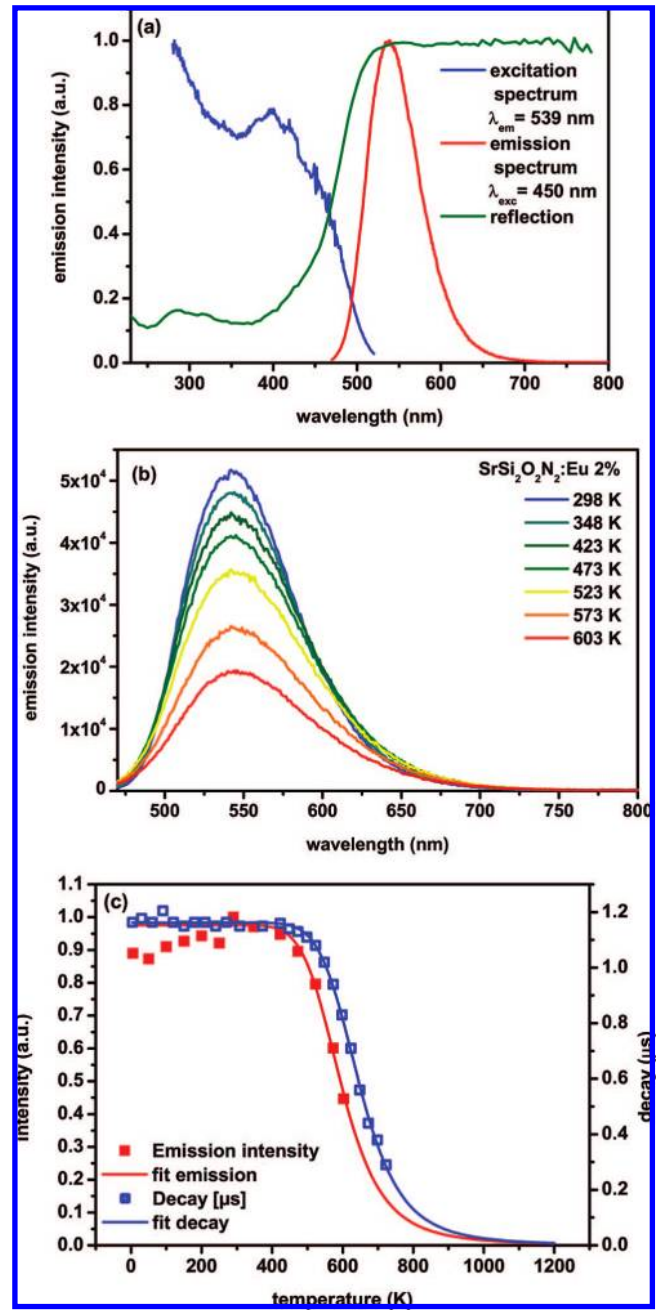

Figure 1. (a) Luminescence excitation (λ_{em} = 539 nm) and emission (λ_{exc} = 450 nm) and diffuse reflection spectrum of $SrSi_2O_2N_2$:Eu 2%, recorded at 298 K; (b) emission spectra of $SrSi_2O_2N_2$:Eu 2% (λ_{exc} = 450 nm) for various temperatures; (c) temperature dependence of the integrated emission intensity and luminescence decay times. The lines through the data points are fits to eq 1.

An important parameter for LED phosphors is the luminescence quenching temperature. This is especially important in high power LEDs where the phosphor temperature can increase up to 450 K. In Figure 1b, the temperature dependence of the Eu^{2+} emission spectra are shown for the sample doped with 2% Eu^{2+}. The integrated intensity as a function of temperature is plotted in Figure 1c. The small increase in emission intensity between 4 and 300 K is not due to an increase in quantum efficiency but is rather due to small changes in the sample alignment and/or to a small

(16) Kechele, J. A.; Oeckler, O.; Stadler, F.; Schnick, W. *Solid State Sci.*, in press.

change in the absorption strength at the excitation wavelength. In addition to monitoring the temperature dependence of the emission intensity, the temperature dependence of the luminescence decay time was also measured. All curves show a close to single exponential decay behavior. The decay time at RT was measured to be 1.15 μs, which is a typical value found for green Eu^{2+} emission.[17,18] The integrated emission intensities and luminescence decay times are plotted as function of temperature in Figure 1c. The lines through the data points represent a fit according to eq 1[6]

$$\tau(T) = \frac{\tau_0}{1 + Ce^{\frac{-E_A}{kT}}}; \quad I(T) = \frac{I_0}{1 + De^{\frac{-E_A}{kT}}} \qquad (1)$$

where $\tau(T)$ and $I(T)$ are luminescence decay time and intensity at temperature T (K), respectively, τ_0 and I_0 the decay time and intensity at low temperatures (only radiative decay), C and D are the rate constants for the thermally activated escape, E_A is the activation energy connected with this process (the energy gap between the lowest energy Eu^{2+} $4f^65d^1$-excited level and the bottom of the conduction band), and k is the Boltzmann constant. The intensity at 4.2 K was set to 1. The experimental data are well-described by eq 1 and the plots were used to determine the temperature at which intensity drops to 50% of its initial value ($T_{50\%}$). For both the temperature dependence of the integrated emission intensity and the luminescence decay time, $T_{50\%}$ for the sample doped with 2% Eu^{2+} is calculated to be around 600 K.

By varying the concentration of Eu^{2+} in the host lattice, the influence of energy migration and energy transfer processes on the (temperature) quenching and the color point can be studied. In Figure 2a, the shift in the emission band to longer wavelengths upon raising the Eu concentration is shown. The dependence of the (room temperature) quantum efficiency and decay time for $Sr_{1-x}Eu_xSi_2O_2N_2$ (x = 0.005−0.16) are shown in Figure 2(b). Decay times are constant around 1 μs for concentrations $x \leq 0.02$ and decrease for higher dopant concentrations. It is well-known that energy migration due to energy transfer between Eu^{2+} ions followed by energy transfer to traps or quenching sites leads to a faster luminescence decay.[1] On the basis of the decrease in the emission intensity and the luminescence lifetime for concentrations greater than 2%, we conclude that the critical concentration for energy migration (x_c) for Eu^{2+} is 0.02. The quantum efficiency is found to have a maximum at $x = 0.02$. One would expect the quantum efficiency to be constant up to the critical concentration and to only decrease, in analogy to the decay time, for higher doping levels. The observation of a maximum at $x = 0.02$ implies the presence of competing absorption processes by nonluminescent defects or impurities. At low Eu^{2+} concentrations (less than 2%), a significant part of the exciting radiation will be absorbed by these impurities or defects and will not result in Eu^{2+} emission, thus explaining the lower quantum efficiencies for the samples with 0.5% Eu. Clearly, the quantum efficiency will depend on the synthesis conditions and for lower Eu concentrations higher quantum yields can be obtained by further improving the synthesis conditions to reduce the number of defects and impurities.

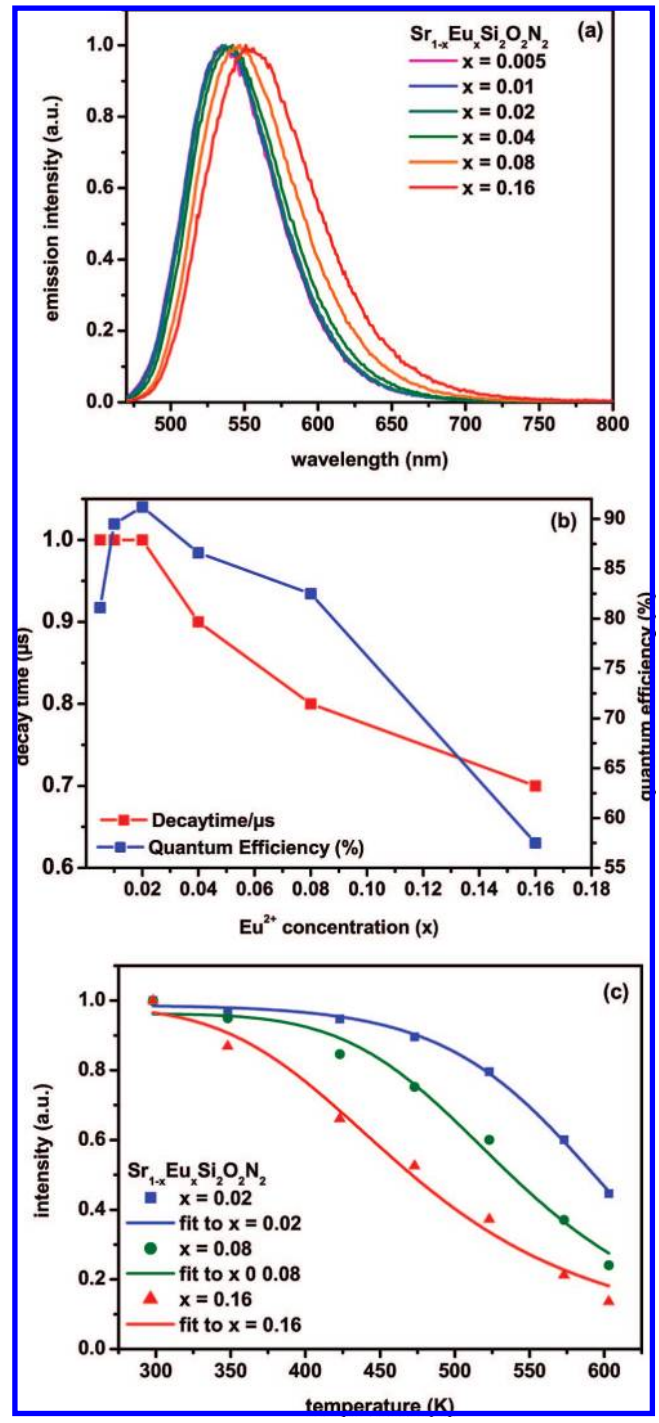

Figure 2. (a) Normalized emission spectra for $Sr_{1-x}Eu_xSi_2O_2N_2$ (x = 0.005−0.16) at RT and excited at λ_{ex} = 450 nm; (b) dependence of the luminescence decay times and quantum efficiency on the concentration of Eu^{2+} in $SrSi_2O_2N_2$:Eu; (c) temperature dependence of the integrated emission intensity (for x = 0.02, 0.08, and 0.16).

Turning to the influence of Eu^{2+} concentration on the color we observe that for concentrations up to 2% Eu^{2+} the color point is almost stable (no shift in the emission spectrum). Upon doping the host lattice with higher amounts of Eu^{2+}, a continuous red shift is observed. There are two possible causes for the shift in color point. First, reabsorption, and

(17) Dorenbos, P. *J. Lumin.* **2003**, *104*, 239.
(18) Poort, S. H. M.; Meijerink, A.; Blasse, G. *J. Phys. Chem. Solids* **1997**, *58*, 1451.
(19) Shannon, R. D. *Acta Crystallogr., Sect. A* **1976**, *32*, 751.

second, energy transfer between different Eu^{2+} sites. In the case of reabsorption, the high energy part of the emission (resonant with the low energy part of the excitation spectrum) is reabsorbed, thus shifting the emission spectrum to the red. In the case of energy transfer between Eu^{2+} ions, energy is transferred to Eu^{2+} ions emitting at lower energy, possibly via multiple energy-transfer steps between Eu^{2+} ions (energy migration). In case of a single type of crystallographic site, energy migration to perturbed Eu^{2+} ions, emitting at lower energies can occur. In the case of multiple crystallographic sites, energy transfer will occur to the Eu ions at sites where the emission is at the lowest energies and a larger spectral shift can be expected at lower Eu-concentrations. To determine which process (energy transfer or reabsorption) is responsible, the concentration dependence of the luminescence lifetime is considered. In the case of (multiple) reabsorption steps, the experimentally observed luminescence lifetime lengthens. The emission of photons is delayed by the reabsorption steps. In the case of energy transfer, the luminescence lifetime is shortened, especially on the shorter wavelength side of the emission band. Because of energy transfer, there are additional decay channels that shorten the lifetime of the excited state. The results show a shortening of the lifetime upon increasing the Eu^{2+} concentration. This indicates that the shift in color point is mainly caused by energy transfer processes, although a contribution from reabsorption cannot be excluded.

The presence of four different crystallographic sites for Sr^{2+} (and thus Eu^{2+}) is in line with the assignment of the observed shift of the color point upon increasing the concentration to energy transfer. The energy will be transferred to the Eu^{2+} ions emitting at longer wavelengths (lower energy) upon increasing the concentration. From structure analysis it is known that of the four crystallographic sites that can be occupied by Eu^{2+}, two sets of two have a similar surrounding.[14] To distinguish between the two types, emission spectra were recorded for a low concentration of 0.5% Eu^{2+} at 4.2 K but no clear differences were observed in the emission spectra recorded for different excitation wavelengths indicating that the emitting d-levels for the different sites are too close in energy to be clearly distinguished, even in low temperature luminescence spectroscopy. Some evidence for the presence of different sites was obtained by comparing the excitation spectra for 480 and 640 nm emission for samples with low Eu^{2+} concentrations. A difference in the region around 300 nm was observed, indicating a difference in the splitting of the $4f^65d^1$ excited states for the different sites. Finally, it should be noted that the relative occupation numbers of the different sites may depend on the Eu concentration and at low Eu concentrations, one type of site may be preferentially occupied (preventing a clear observation of Eu luminescence from the different sites), whereas at higher concentrations, other sites are also occupied. However, in view of the similarity of the four sites, a large preference of Eu for one of the sites is not expected. On the basis of the observed red-shift and the shortening of the emission lifetime (especially on the short wavelength side of the emission band) upon raising the Eu concentration, the spectral shift is assigned to energy transfer between Eu ions.

Table 1. Color Coordinates (x and y), Quantum Efficiency (%), and Maximum Emission Wavelength, All at RT, Quenching Temperature $T_{50\%}$ (K), All for Excitation Wavelength of 450 nm for $Sr_{1-x}Eu_xSi_2O_2N_2$ ($x = 0.005-0.16$)

composition	x	y	QE (%)	λ_{max} (nm)	$T_{50\%}$ (K)
$Sr_{0.995}Eu_{0.005}Si_2N_2O_2$	0.330	0.621	81	535	
$Sr_{0.99}Eu_{0.01}Si_2N_2O_2$	0.330	0.621	90	535	
$Sr_{0.98}Eu_{0.02}Si_2N_2O_2$	0.337	0.619	91	538	600
$Sr_{0.96}Eu_{0.04}Si_2N_2O_2$	0.352	0.611	87	541	
$Sr_{0.92}Eu_{0.08}Si_2N_2O_2$	0.384	0.590	83	546	537
$Sr_{0.84}Eu_{0.16}Si_2N_2O_2$	0.419	0.562	58	554	471

Most probably, energy transfer to Eu ions on crystallographic sites where the emission is situated at slightly longer wavelengths is responsible for the red shift, whereas transfer to Eu ions on slightly perturbed sites emitting at longer wavelengths can also contribute to the red shift observed upon raising the Eu concentration.

Figure 2a shows the emission spectra for $SrSi_2O_2N_2$ doped with various amounts of Eu^{2+}. It shows that varying the Eu^{2+} concentration can be used for tuning of the color point. The spectral shift that can be realized is 8 nm (band maximum shifts from 539 nm at 0.005 Eu^{2+} to 547 nm at 0.16 Eu^{2+}). The shift in emission color is however accompanied by a reduction in the quantum efficiency due to concentration quenching. At room temperature the quantum efficiency for the $x = 0.16$ sample has dropped to 57%. This restricts the application of higher doped $SrSi_2O_2N_2$:Eu^{2+} phosphors. The thermal quenching behavior is also affected by increasing the concentration. Because of thermal broadening at elevated temperatures the spectral overlap between excitation and emission band increases upon raising the temperature. This leads to faster energy migration and stronger concentration quenching. Also, there may be a difference in luminescence quenching temperature for Eu ions on the different sites in which case energy transfer to Eu ions on sites with a lower quenching temperature may also contribute to the observed lower quenching temperature at the highest Eu concentrations. The change in quenching temperature is limited and the thermal quenching temperatures for the highest dopant concentrations are still acceptable ($T_{50\%}$ is 537 and 471 K for 8% and 16% Eu^{2+}, respectively). Figure 2c shows the emission intensities of the samples containing 2, 8, and 16% Eu^{2+} as function of temperature. Intensities at 300 K were each normalized to unity. The thermal quenching of 4f−5d luminescence of 2% Eu^{2+} in $SrSi_2O_2N_2$ is marginal at typical LED operation temperatures ($T_{50\%} = 600$ K). It also exhibits a high quantum efficiency (above 0.9), which makes this phosphor suitable for the use in pc-LEDs as proposed in ref 13. In Table 1, the luminescence properties for $Sr_{1-x}Eu_x$-$Si_2O_2N_2$ for the different Eu^{2+} concentrations are summarized.

3.3. $Sr_{0.98-x-y}Ca_xBa_yEu_{0.02}Si_2O_2N_2$. *3.3.1. $Ca_{0.98}Eu_{0.02}Si_2O_2N_2$ and $Ba_{0.98}Eu_{0.02}Si_2O_2N_2$.* A second method to shift the position of the Eu^{2+} emission band is to replace part of the Sr^{2+} ions with a larger (Ba^{2+}) or smaller (Ca^{2+}) cations. To understand the influence of partial replacement of Sr^{2+} by the other alkaline earth ions, it is good to compare the luminescence spectra of Eu^{2+} in the pure host lattices for all three alkaline earth ions. The ionic radii of the ions (in six coordination) are 115 pm for Ca^{2+}, 131 pm for Eu^{2+}, 132

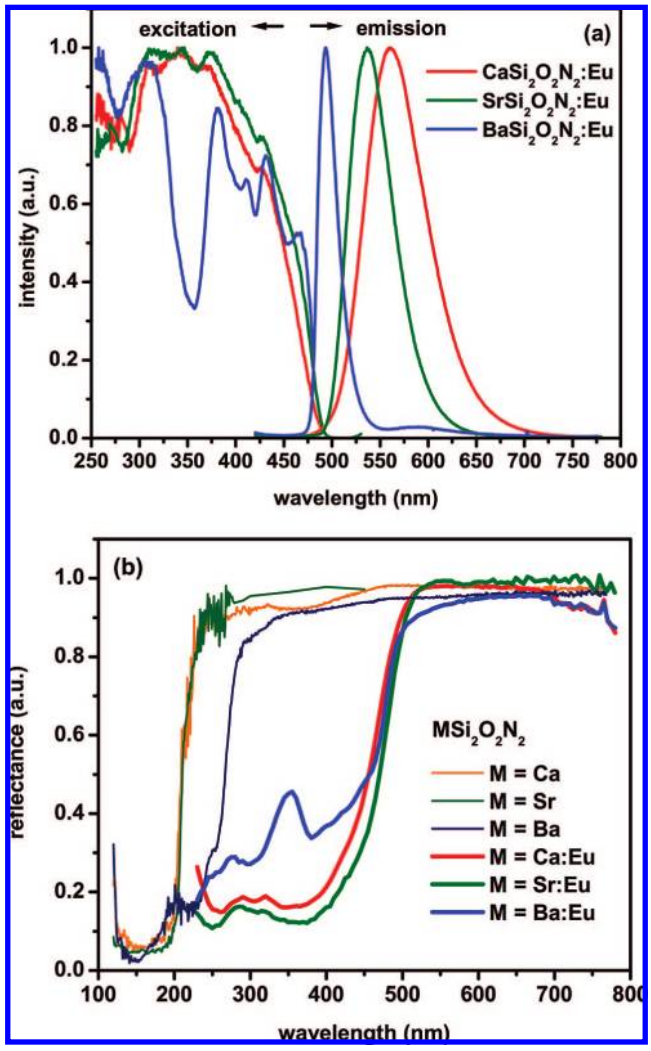

Figure 3. (a) Excitation and emission spectra of $CaSi_2O_2N_2$, $SrSi_2O_2N_2$, and $BaSi_2O_2N_2$, each doped with 2% Eu^{2+} taken at 4 K; emission spectra were taken at 450 nm excitation wavelength; excitation spectra were taken at the emission maxima (see also Table 2); (b) diffuse reflection spectra of undoped and 2% Eu^{2+}-doped $CaSi_2O_2N_2$, $SrSi_2O_2N_2$, and $BaSi_2O_2N_2$.

pm for Sr^{2+}, and 149 pm for Ba^{2+}.[19] In Figure 3a, the excitation and emission spectra are shown of the three compositions $BaSi_2O_2N_2$, $SrSi_2O_2N_2$, and $CaSi_2O_2N_2$ each doped with 2 at % Eu^{2+} measured at low temperature (4 K). The emission maxima are at 494, 537, and 560 nm for the Ba, Sr, and Ca compounds, respectively. The onset of the $4f^65d^1$ band in the excitation spectra shifts to higher energies going from Ba to Ca. The room temperature luminescence spectra of these compounds have also been reported in ref 10. The results are similar, but differences in the bandwidth and shape have been found. No shoulder on the long wavelength side is observed in the presently reported spectra, which is likely to originate from a better phase purity and/or crystallinity.

The shift to higher energies of the 4f−5d emission from Ca to Ba is due to two effects. First, the crystal field splitting of the d-manifold is smaller for Eu^{2+} on a larger cation site. As a result, the position of the lowest energy 5d state (the emitting state) shifts to higher energies from Ca^{2+} to Sr^{2+} to Ba^{2+} host lattices, assuming that the barycenter is not affected. The energy of the barycenter is lower for Eu^{2+} in a more covalent host lattice. The covalency of the oxonitridosilicates is expected to be similar. The silicate layers in the three structures are almost the same as is the electronegativity of the alkaline earth cations. The reduction in energy (barycenter) of the Eu 5d state by covalent bonding is mainly determined by the interaction with the surrounding anions (oxygen and nitrogen), which is expected to be similar in view of the similarities in the layered structures. A second origin for the shift of the emission to lower energies from Ba to Sr to Ca is the Stokes shift. The Stokes shift is largest for the Eu^{2+} emission in the Ca compound and smallest in the Ba compound. The width of the emission band also becomes larger as the Stokes shift increases. These observations are typical for the luminescence of Eu^{2+} in (isostructural) alkaline earth compounds. The results are explained by considering the relaxation in the $4f^65d^1$ excited state. There is increasing evidence that, contrary to most luminescent ions and molecules, the equilibrium distance in the f−d excited states of lanthanide ions can be smaller than for the ground state.[20−25] Both ab initio (cluster) calculations and experimental results for Ce^{3+}, Sm^{2+}, and Eu^{2+} indicate that the bonding in (some) $4f^{n-1}5d$ states of Sm^{2+}, Eu^{2+}, and Ce^{3+} may be stronger than in the ground state. As a result, the change in equilibrium distance (due to contraction!) in the $4f^65d$ excited state is largest when Eu^{2+} is substituted on a small cation site (like Ca^{2+}), which will result in the largest relaxation and shift of the parabolas in the configurational coordinate diagram. On the other hand, when Eu^{2+} replaces a large cation (like Ba^{2+}) the reduction of the distance between Eu^{2+} and the coordinating anions will be unfavorable since the site is already too large for Eu^{2+}. The small relaxation results in a small shift of the parabolas in the configurational coordinate diagram, which is reflected in the luminescence spectra by a small Stokes shift, narrow bands and a high luminescence quenching temperature. Even though the compounds investigated are not isostructural, the structures are similar and the differences in the luminescence spectra for Eu^{2+} in the three compounds can be explained by the model discussed above. The temperature quenching for the Eu^{2+} emission will be discussed below.

A second difference is that the excitation spectrum for the Eu^{2+} emission in $BaSi_2O_2N_2$ shows relatively narrow bands

Table 2. Summary of Luminescence Properties for $CaSi_2O_2N_2$, $SrSi_2O_2N_2$, and $BaSi_2O_2N_2$, Each Doped with 2% Eu^{2+} (spectral properties determined from room-temperature spectra)

property	$CaSi_2O_2N_2$	$SrSi_2O_2N_2$	$BaSi_2O_2N_2$
emission max. (nm)	560	537	494
absorp. max. (nm)	355	360	380
onset absorp. undoped (nm)	210	210	260
Stokes shift[a] (eV)	0.64	0.43	0.14
fwhm (eV)	0.29	0.23	0.12
onset quenching (decay) (K)	380	450	420
quenching temp. $T_{50\%}$ (K)	440	600	600

[a] As determined from the emission and excitation maxima. A more careful analysis for the low temperature spectra will yield smaller Stokes shifts, see also ref 22.

(20) Barandiarán, Z.; Seijo, L. *J. Chem. Phys.* **2003**, *119*, 3785.
(21) Barandiarán, Z.; Edelstein, N. M.; Ordejón, B.; Ruiperez, F.; Seijo, L. *J. Solid State Chem.* **2005**, *178*, 464.
(22) Meijerink, A.; Blasse, G. *J. Lumin.* **1989**, *43*, 283.
(23) Pascual, J. L.; Barandiaran, Z.; Seijo, L. *Phys. Rev. B* **2007**, *76*, 104109.
(24) Barandiaran, Z.; Seijo, L. *Theor. Chem. Acc.* **2006**, *116*, 505.
(25) Ruiperez, F.; Seijo, L.; Barandiaran, Z. *J. Chem. Phys.* **2005**, *122*, 234507.

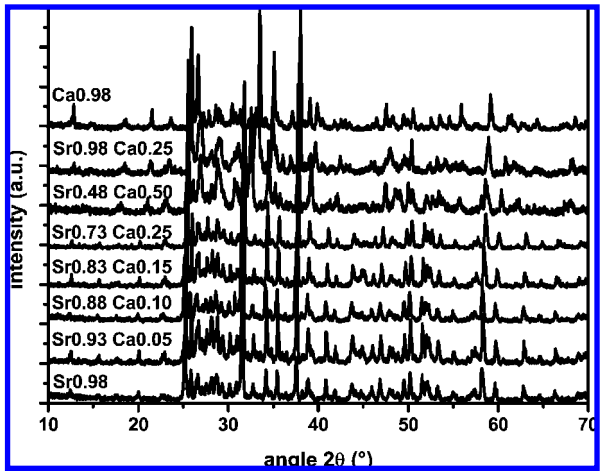

Figure 4. XRD patterns of $Sr_{0.98-x}Ca_xSi_2O_2N_2$:Eu 2% ($x = 0-1$) at RT.

and structure that is explained by the splitting of the $4f^6$ core in the $4f^65d^1$ excited state into the different ^7F_J components.[22] The width of the lowest energy excitation band (extending between 375 and 475 nm) is about 6000 cm^{-1}, close to the theoretical ^7F_J splitting of 5200 cm^{-1}. The fact that the structure cannot be observed for Eu^{2+} in the Ca- and Sr-compound is probably due to the fact that in these compounds there are four different crystallographic sites, each with slightly different excitation spectra. The overlapping spectra of the four different types of Eu^{2+} ions obscures the fine structure. In addition, the larger width of the excitation bands (due to the larger relaxation in the excited-state as discussed above) will also contribute to the absence of a well-resolved structure in the excitation spectra for Eu^{2+} in $CaSi_2O_2N_2$ and $SrSi_2O_2N_2$. The diffuse reflection spectra of the three compositions each doped with 2% Eu^{2+} are shown in Figure 3b. The spectra are consistent with the excitation spectra. To determine the bandgap of the three alkaline earth oxonitridosilicates, diffuse reflection spectra were also recorded for the undoped compounds. Figure 3b depicts the reflection spectra. The absorption onset is at 260 nm (4.8 eV) for $BaSi_2O_2N_2$ and 210 nm (5.9 eV) for $CaSi_2O_2N_2$ and $SrSi_2O_2N_2$. In Table 2, the luminescence properties are collected for comparison.

3.3.2. $Sr_{0.98-x}Ca_xEu_{0.02}Si_2O_2N_2$ ($0 \le x \le 0.98$). A high flexibility in the color point tuning may be achieved by continuously varying the fraction x in $Sr_{0.98-x}Ca_xEu_{0.02}Si_2O_2N_2$ between 0 and 1. It is known from refs 14 and 15 that the structures for the Ca and the Sr compounds are similar although not isotypic. To investigate the structural changes upon increasing the Ca-content, we recorded X-ray powder diffractograms. In Figure 4, the diffractograms are shown. The overall pattern does not change up to a Ca fractions of 0.5. Upon increasing the Ca content, the diffraction peaks shift to larger angles. This indicates that solid solutions are formed. The shift of the diffraction peaks to larger angles is consistent with a contraction of the lattice parameters due to the smaller ionic radius of Ca^{2+} in comparison to Sr^{2+}. For Ca^{2+} fraction of 0.5 and higher, a heterogeneous mixture of the two structures rather than a solid solution was observed. Some reflections cannot be attributed to these phases and might result from an unknown compound.

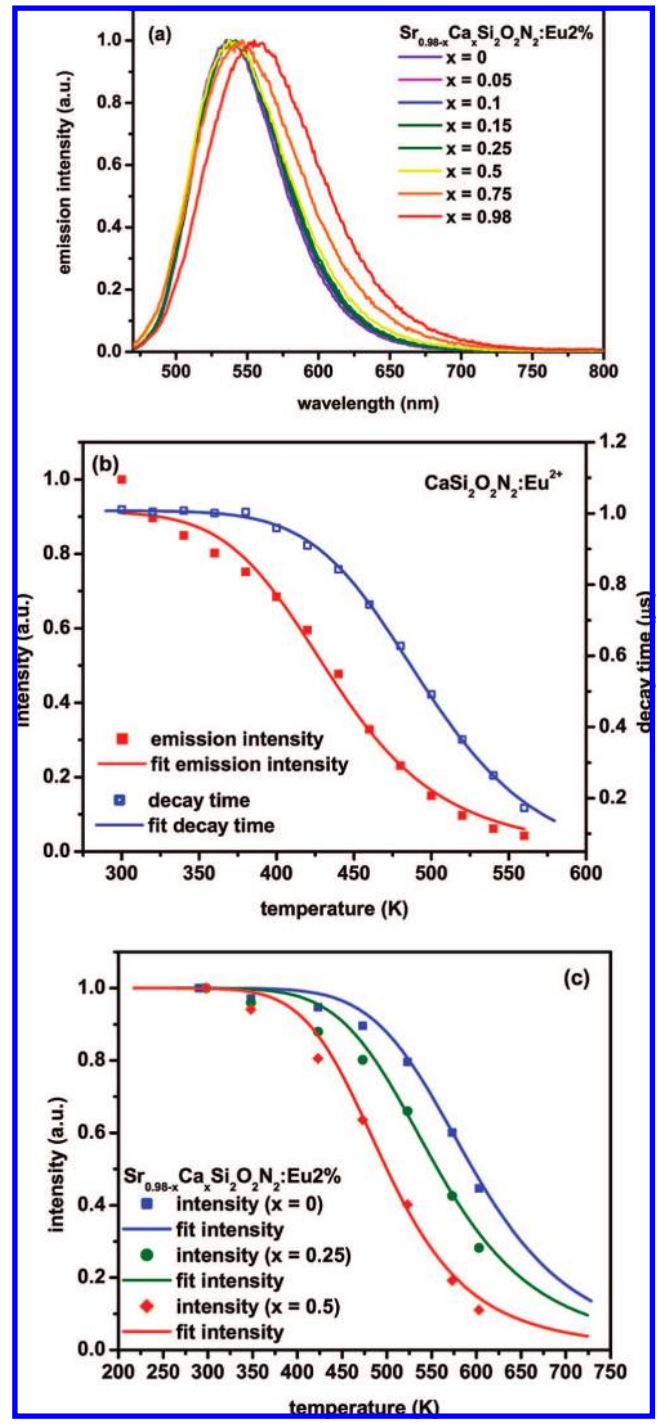

Figure 5. (a) Normalized emission spectra for $Sr_{0.98-x}Ca_xSi_2O_2N_2$:Eu 2% ($x = 0-0.98$) at RT ($\lambda_{ex} = 450$ nm); (b) temperature dependence of the integrated emission intensity and luminescence decay times in $CaSi_2O_2N_2$:Eu 2% ($\lambda_{ex} = 450$ nm); (c) temperature dependence of the integrated emission intensity $Sr_{0.98-x}Ca_xSi_2O_2N_2$:Eu 2% ($x = 0$, 0.25, 0.5; $\lambda_{ex} = 450$ nm). The lines through the data points are fits to eq 1.

In Figure 5a, the Eu^{2+} emission spectra are shown for various compositions. The emission band continuously shifts to longer wavelengths as the fraction of Ca^{2+} is increased. For the highest Ca fractions (0.5 and higher) also emission from Eu^{2+} in the second phase may contribute to the spectral shift. Along with the spectral shift, the width of the emission band and the Stokes shift increase. By varying the molar Ca:Sr ratio, the maximum of the emission band can be tuned precisely to any wavelength between 537 and 560 nm.

Table 3. Color Coordinates (*x* and *y*), Quantum Efficiency (%), and Maximum Emission Wavelength, All at RT, Quenching Temperature $T_{50\%}$ (K), All for Excitation Wavelength of 450 nm for $Sr_{0.98-x}Ca_xSi_2O_2N_2$:Eu 2% ($x = 0-0.98$)

composition	*x*	*y*	QE (%)	λ_{max} (nm)	$T_{50\%}$ (K)
$SrSi_2N_2O_2$:Eu 2%	0.337	0.619	91	538	600
$Sr_{0.93}Ca_{0.05}Si_2N_2O_2$:Eu 2%	0.342	0.616	89	538	
$Sr_{0.88}Ca_{0.10}Si_2N_2O_2$:Eu 2%	0.345	0.614	93	538	
$Sr_{0.83}Ca_{0.15}$ $Si_2N_2O_2$:Eu 2%	0.349	0.611	93	536	
$Sr_{0.73}Ca_{0.25}Si_2N_2O_2$:Eu 2%	0.351	0.608	93	542	557
$Sr_{0.48}Ca_{0.50}Si_2N_2O_2$:Eu 2%	0.354	0.601	92	543	500
$Sr_{0.23}Ca_{0.75}$ $Si_2N_2O_2$:Eu 2%	0.378	0.581	81	546	
$CaSi_2N_2O_2$:Eu 2%	0.419	0.556	76	555	440

The thermal quenching of the luminescence is important for applications. To study the influence of the replacement of Sr by Ca on the luminescence quenching, the intensity of the Eu^{2+} emission and the luminescence decay time were measured as a function of temperature for $CaSi_2O_2N_2$ with 2% Eu^{2+}. In Figure 5b, the results are shown. The luminescence decay time and the emission intensity steadily decrease between 300 and 600 K. The decay time of 1 μs at RT is typically found for Eu^{2+}-activated phosphors emitting in the green spectral region.[17,18] The plot of the decay times and the emission intensities as a function of temperature (Figure 5b) shows that the onset of the thermal quenching is around 300 K and $T_{50\%}$ is around 440 K. One would expect the temperature dependence of the intensity and the luminescence decay time to be the same, both being affected in a similar manner by thermally induced nonradiative decay processes. The results show that the intensity starts to drop in a lower temperature range than the decay time. Possibly, this can be due to thermally activated nonradiative relaxation from a higher f−d state, before thermal equilibrium is reached. In spite of the discrepancy between the temperature dependence of the luminescence lifetime and intensity, it is clear that the luminescence quenching temperature is much lower than for the Eu^{2+} emission in $Sr_{0.98}Eu_{0.02}Si_2O_2N_2$ and that it is too low for an application of $Ca_{0.98}Eu_{0.02}Si_2O_2N_2$ in high-power LEDs. For two intermediate compositions, the temperature dependence of the emission intensity was also measured. The results are shown in Figure 5c. For the sample with $x = 0.25$ the quenching temperature is 557 K and for $x = 0.5$ $T_{50\%}$ is 500 K. This shows that also the quenching temperature of the emission gradually decreases upon raising the fraction of Ca.

For all compositions the luminescence quantum efficiency was determined at 300 K. For values of *x* between 0 and 0.5 the quantum efficiency at room temperature is high, better than 90%. For the samples with $x = 0.75$ and $x = 1.0$ a lower quantum efficiency is measured (81 and 76%, respectively). All the results are tabulated in Table 3. The table shows that the luminescence properties gradually change from those of $Ca_{0.98}Si_2O_2N_2$:Eu 2% to those of $Sr_{0.98}Si_2O_2$:Eu2%. Up to a fraction of $x = 0.5$ the quantum efficiency and thermal quenching temperature are high and meet the criteria for application in pc-LEDs. Above $x = 0.5$ the quantum efficiency and luminescence quenching temperature drop to values that are too low for commercial application. On this basis, one can conclude that Ca-doping can be used for color point tuning in $Sr_{0.98}Si_2O_2N_2$:Eu 2% up to a fraction of 0.5. Note, however, that the spectral shift that can be achieved is limited (from 538 nm for $x = 0$ to 543 nm for $x = 0.5$).

3.3.3. $Sr_{0.98-x}Ba_xEu_{0.02}Si_2O_2N_2$ ($0 \le x \le 0.98$). The Eu^{2+} emission band for $BaSi_2O_2N_2$:Eu is shifted to shorter wavelengths (495 nm) in comparison to the Eu^{2+} emission band for $SrSi_2O_2N_2$:Eu (538 nm). To investigate the influence of partial replacement of Sr by Ba, a concentration series was investigated for $Sr_{0.98-x}Ba_xEu_{0.02}Si_2O_2N_2$:Eu 2% with $x = 0.05$, 0.1, 0.15, 0.25, 0.5, 0.75, and 1. In Figure 6a, the emission spectra are shown. Up to a concentration of $x = 0.75$ there is a continuous redshift of the emission band, from 538 nm for $x = 0$ to 564 nm for $x = 0.75$. However, for $x = 1$ there is a sudden blue shift of the emission band maximum to 495 nm.

To understand this unexpected behavior, the X-ray diffraction patterns are considered. The XRD patterns for the various compositions are depicted in Figure 7. The patterns show that even for small amounts of Ba-doping, the reflections shift to smaller angles. This is accompanied by changes in the intensity ratios between the strongest reflections. The shifts to smaller angles shows that the lattice parameters increase upon replacing part of the Sr ions with the (larger) Ba ions, as expected for a solid solution of Sr and Ba. Intensity changes can be ascribed to differences in the scattering power between Sr and Ba and to differently overlapping reflections when the peaks shift due to changes in the unit cell parameters. A drastic change is observed between the XRD patterns for $x = 0.75$ and $x = 1$: the XRD pattern for $x = 1$ corresponds to a different crystal structure, the structure of $BaSi_2O_2N_2$ (as discussed in section 3.1). On the basis of the XRD patterns we conclude that upon replacing Sr by Ba, the crystal structure of the Sr compound is preserved up to a (weighed in) fraction of 0.75 for Ba^{2+} in the starting materials. The transition to solid solutions with the Ba-phase occurs for a fraction between 0.75 and 1. The luminescence measurements show that for the solid solutions $Sr_{0.98-x}Ba_xSi_2O_2N_2$:Eu 2% the emission shifts to longer wavelengths as the fraction *x* of Ba increases. This behavior is opposite to the expected blue shift in view of the larger lattice parameters due to the larger size of Ba^{2+} ion. The redshift may be explained by the fact that the (Sr,Eu)$Si_2O_2N_2$ structure is preserved while a part of the Sr^{2+} ions is replaced by the larger Ba^{2+} ions. To accommodate these larger cations, the distances between Sr^{2+} (or Eu^{2+}) and the anions may not increase or even become slightly smaller, thus increasing the crystal field splitting, causing a red shift of the emission. Only after the transition (for $x = 1$) to a different crystal structure in which the cation−anion distances are larger (determined by the Ba^{2+} ion) the substitution of Eu^{2+} on this (larger) cation site will result in a blue-shifted emission due to a smaller crystal field splitting and a smaller relaxation in the $4f^65d^1$ excited-state for Eu^{2+}. To validate this hypothesis, and to explain the difference in behavior with the Ca−Sr system, where a blue shift is observed upon replacing the smaller Ca^{2+} ion by the larger Sr^{2+} ion, we consider the crystal structures for the three compositions.[16] The cation coordination in $CaSi_2O_2N_2$ and (Sr,Eu)$Si_2O_2N_2$ is a trigonal prism and is quite similar. In $BaSi_2O_2N_2$, the

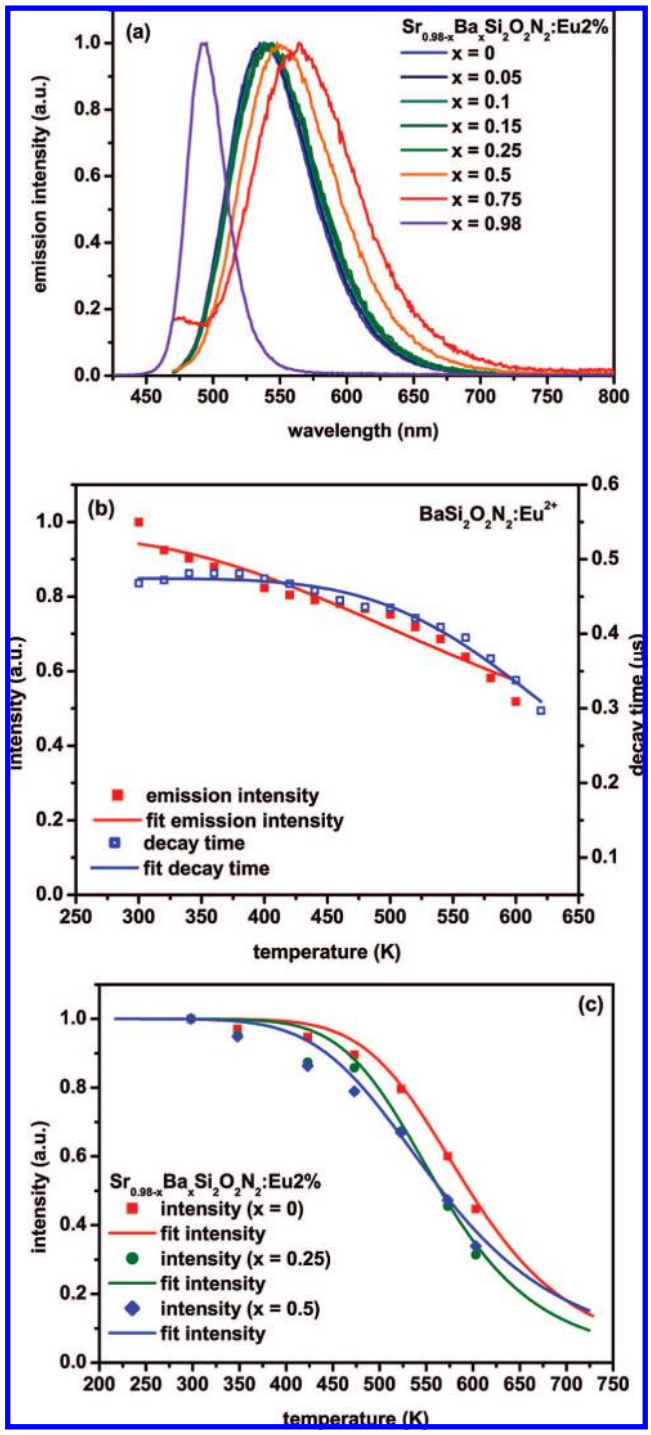

Figure 6. (a) Normalized emission spectra for $Sr_{0.98-x}Ba_xSi_2O_2N_2$:$Eu_{0.98}$ ($x = 0-0.98$) at RT ($\lambda_{ex} = 450$ nm); (b) temperature dependence of the integrated emission intensity and luminescence decay times in $BaSi_2O_2N_2$: Eu 2%; (c) temperature dependence of the integrated emission intensity $Sr_{0.98-x}Ba_xSi_2O_2N_2$:Eu 2% ($x = 0$, 0.25, 0.5). The lines through the data points are fits to eq 1.

cation coordination is different, which indicates that the trigonal prism is too small for Ba and, upon addition of Ba in the Sr compound, the trigonal prim is either enlarged or the coordination is locally changed to 8 (as it is in the Ba compound) and might thus explain the shrinking of the neighboring Sr or Eu sites. Only upon transition of the structure to the $BaSi_2O_2N_2$ phase (for the pure Ba compound) will the Eu substitute for the Ba^{2+} ion in this structure on the large 8-coordinated site, explaining the blue shift

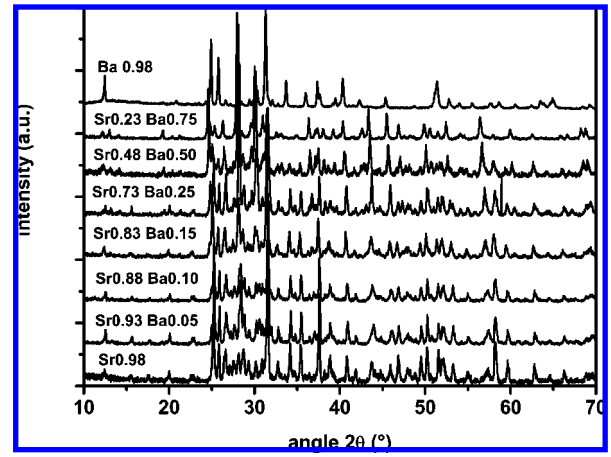

Figure 7. XRD patterns of $Sr_{0.98-x}Ba_xSi_2O_2N_2$:Eu 2% ($x = 0-0.98$) at RT.

observed for the Eu^{2+} emission in this compound. In the case of $CaSi_2O_2N_2$, addition of Sr will lead to an expansion of all cation polyhedra, explaining the continuous blue shift of the Eu emission upon increasing the Sr fraction. On the basis of the difference in coordination of the divalent cation in $CaSi_2O_2N_2$ and $SrSi_2O_2N_2$ on the one hand and in $BaSi_2O_2N_2$ on the other hand, we can understand the difference in the direction of the shift of the Eu emission band upon substitution of a smaller by a larger cation.

To evaluate the potential as color converter in LEDs the thermal quenching behavior has been measured for a number of compositions. For the Eu^{2+} emission in $Ba_{0.98}Si_2O_2N_2$:Eu 2%, both the emission intensity and the decay times between 300 and 600 K were measured. All decay curves were found to be single exponential. In Figure 6b, emission intensity and decay time are plotted as function of temperature. The intensity at 300 K was normalized to 1. The room temperature decay time was found to be 0.47 μs. This decay time is shorter than expected for a radiative decay for Eu^{2+} emission with a maximum at 495 nm.[17,18] The shorter lifetime may be explained by the low quantum efficiency at room temperature. The quantum yield is only 71%, indicating that there is already nonradiative decay at 300 K. If this is the case, the lifetime of 0.47 μs contains a radiative and a nonradiative component and the radiative decay rate can estimated to be 0.65 μs which is slightly shorter than the expected value.[18] The results in Figure 6b show that the onset of thermal quenching is above 300 K and the value of $T_{50\%}$ for both curves is found to be around 600 K. However, the fact that the QE at 300 K is only 0.71 is unfavorable for application of $Ba_{0.98}Si_2O_2N_2$:Eu 2% in white light LEDs, where the industrial standard for the QE is >0.9.

To investigate the luminescence temperature quenching for the mixed (Sr,Ba) compounds, the temperature dependence of the emission intensities for the samples containing 25 and 50% Ba^{2+} were measured. The results are shown in Figure 6c. For comparison the temperature dependence of the emission intensity of the pure Sr compound is also included. The intensity at 300 K was normalized to unity for all three samples. From Figure 6c, it is clear that the quenching temperature $T_{50\%}$ is reduced from 600 K for $SrSi_2O_2N_2$:Eu to 560 K for the two Ba-doped materials.

Table 4. Color Coordinates (*x* and *y*), Quantum Efficiency (%), and Maximum Emission Wavelength, All at RT, QuenchingTemperature $T_{50\%}$ (K), All for Excitation Wavelength of 450 nm for $Sr_{0.98-x}Ba_xSi_2O_2N_2$:Eu 2% ($x = 0-0.98$)

composition	*x*	*y*	QE (%)	λ_{max} (nm)	$T_{50\%}$ (K)
$SrSi_2N_2O_2$:Eu 2%	0.337	0.619	91	538	600
$Sr_{0.93}Ba_{0.05}Si_2N_2O_2$:Eu 2%	0.343	0.614	91	538	
$Sr_{0.88}Ba_{0.10}Si_2N_2O_2$:Eu 2%	0.351	0.610	90	539	
$Sr_{0.83}Ba_{0.15}Si_2N_2O_2$:Eu 2%	0.358	0.606	89	544	
$Sr_{0.73}Ba_{0.25}Si_2N_2O_2$:Eu 2%	0.361	0.602	79	544	560
$Sr_{0.48}Ba_{0.5}Si_2N_2O_2$:Eu 2%	0.401	0.573	91	548	560
$Sr_{0.23}Ba_{0.75}Si_2N_2O_2$:Eu 2%	0.434	0.528	66	564	
$BaSi_2N_2O_2$:Eu 2%	0.076	0.440	71	495	600

These quenching temperatures are high enough for application in HP-LEDs where the maximum temperature of the phosphor is between 450 and 500 K. The quantum efficiencies at RT for the Eu^{2+} emission in the mixed Ba−Sr compositions are also high (∼90%). This shows that small amounts of Ba^{2+} doped into $SrSi_2O_2N_2$:Eu are useful for tuning the color point. The shifting of the color point can be achieved while preserving a high quantum efficiency and a high thermal quenching. The spectral range over which the emission maximum can be tuned is 538−548 nm. Table 4 contains a summary of emission maxima, color points, quantum efficiencies, and thermal quenching data on $Sr_{0.98-x}Ba_xSi_2O_2N_2$:Eu 2%.

4. Conclusion

The ability to tune the emission color of a luminescent material is of great importance for practical applications. Here the color tuning for the efficient oxonitridosilicate phosphor $SrSi_2O_2N_2$:Eu^{2+} is reported with a focus on the use of this material in high power white light LEDs. To change the color of the emission, we followed two concepts: (1) varying the concentration of the Eu^{2+} dopant and (2) changing the host lattice composition by replacing Sr^{2+} with either Ca^{2+} or Ba^{2+}.

Upon raising the Eu^{2+} concentration above 2%, a red shift in the emission is observed from 535 nm (0.5% Eu^{2+}) to 554 nm (16% Eu^{2+}). This is ascribed to energy migration and energy transfer between the dopant ions. Increasing the concentration of Eu^{2+}, however, also results in a decrease of the quantum efficiency and luminescence quenching temperature, which makes this concept not suitable for color tuning aimed at application in white light LEDs.

The concept of color tuning by changing the host lattice was found to be very promising. Replacing part of the host lattice cation Sr^{2+} with Ca^{2+} shows that the crystal structure is preserved up to 50% of ion exchange. A red shift in emission is observed while retaining the high (90%) quantum efficiency. The luminescence quenching temperature is however lower for the Eu^{2+} emission in the mixed (Sr,Ca) compounds. Admixture of Ba^{2+} to the host lattice shows an unexpected red shift of the Eu^{2+} emission. For the mixed composition with up to 50% Ba^{2+}, the high quantum efficiency and a high thermal quenching temperature are maintained for the Eu^{2+} luminescence. On this basis, Ba^{2+} substitution is a promising method for shifting the emission of $SrSi_2O_2N_2$:Eu to longer wavelengths.

Acknowledgment. The authors thank Petra Huppertz, Henning Ohland, and Detlef U. Wiechert for assistance in the optical and thermal characterization and Dr. Peter Schmidt and Dr. Andreas Tücks (all at Philips Technologie GmbH, Aachen) as well as Florian Barth, Florian Stadler, and Juliane A. Kechele (all at Department of Chemistry and Biochemistry, Ludwig-Maximilians-Universität München) for valuable discussions. Financial support by the Fonds der Chemischen Industrie (FCI), Germany, is gratefully acknowledged.

CM802394W